

Anatomical Variations of the Canalis Sinuosus: A CBCT Study

Hatice Tetik¹ , Zühre Akarslan² 

¹ İzmir Training Dental Hospital, İzmir, Türkiye

² Gazi University, Faculty of Dentistry, Department of Oral and Maxillofacial Radiology, Ankara, Türkiye.

Correspondence Author: Hatice Tetik

E-mail: haticetetik94@gmail.com

Received: 27.02.2024

Accepted: 20.07.2024

ABSTRACT

Objective: Canalis sinuosus (CS) is a bony canal separated from the infraorbital nerve containing the anterior superior alveolar vessel-nerve bundle. This study aimed to assess the anatomical variations of the canalis sinuosus from cone-beam computed tomography (CBCT) images.

Methods: CBCT images of 568 patients (328 females and 240 males; aged between 18 and 81 years old) were evaluated retrospectively. Axial, sagittal, coronal, and cross-sectional images with 0.5 mm slice thicknesses were used to evaluate the presence of CS and associated accessory canal (AC).

Results: Bilateral CS was detected in the entire sample (n=568, 100%). A total of 340 ACs were detected, including at least one AC in 41.9% of the patients. The median value of AC diameter was calculated as 0.89 mm both for females and males. ACs were found in 135 females and in 103 males. One up to five ACs were found per patient. However, the majority of the patients had one AC. ACs were mostly located at tooth region 11 (17.9%) and tooth region 12 (16.4%). Only 59.71% of ACs had a radiographically observed foramen.

Conclusion: In conclusion, all patients had CS and ACs were in nearly half of the patients. Knowledge about these structures aid to correct radiographic diagnosis of these canals and minimize the risk of complications during surgical procedures.

Keywords: Canalis sinuosus, cone-beam computed tomography, maxilla, maxillary nerve, radiology

1. INTRODUCTION

Two-dimensional conventional imaging methods, such as periapical and panoramic radiography, may be insufficient in the diagnosis for because of superposition, distortion, and magnification. Cone-beam computed tomography (CBCT) is one of the important advances in imaging the maxillofacial region (1). CBCT is one of the preferred imaging methods in dentistry because it shows hard tissues well, allows one-to-one measurements, and achieves images with a lower radiation dose compared to medical computed tomography (2).

Surgical operations are commonly performed in the maxillary anterior region (3). Vascular damage causes a risk of bleeding and nerve damage can significantly affect the patient's quality of life due to hyperesthesia, paraesthesia, or pain (4,5). Therefore, the major neurovascular structures and anatomical variations in this region should be well known. One of the anatomical structures that have not been sufficiently investigated in this region is canalis sinuosus (CS).

CS was first described by Frederic Wood Jones in 1939 as a bony canal of approximately 2 mm in diameter, separating from the infraorbital nerve (ION) and running beside the nasal cavity, containing nerve and blood vessels (6). It was named CS because of its double-curved course. CS runs forward and downward in the inferior wall of the orbita, lateral to the infraorbital canal. Afterwards, it passes under the infraorbital foramen and curves medially toward the anterior wall of the maxillary sinus. It then follows the inferior edge of the pyriform aperture and opens lateral to the nasal septum in front of the incisive canal (6). This canal, with a course of approximately 55 mm in the maxilla, contains the anterior superior alveolar nerve (ASAN) and vessels of the same name (7). Although CS is a normal anatomical structure, the accessory canal (AC) continuing in the anterior maxilla are not well known.

CS and AC may not be adequately visualized on conventional radiographs. The superposition of AC on tooth roots may

mimic periapical lesion (8) and root resorption (9-11), resulting in misdiagnosis. Implants may cause pain due to their association with CS (12-14) and traumatic neuromas may originate from ASAN (15,16). Also, the maxillary bone anterior to the CS is thin, therefore in midface fractures, the integrity of the CS may be compromised, and the ASAN may become more susceptible to injury (17). Therefore, being aware of the course and anatomical variations of CS is particularly important in terms of diagnosis and treatment planning. Thus, we aimed to evaluate the anatomical variations of CS from CBCT images.

2. METHODS

The study was conducted by the principles defined in the Declaration of Helsinki, including all regulations and revisions. Access to the data used was restricted to the principal researcher only. The Ethical Committee of the University approved this work (date: 07.01.2020 number: 91610558-604.01.02-). The CBCT images of patients who applied the Department of Oral and Maxillofacial Radiology between 2015 and 2018 for various dental reasons were evaluated retrospectively.

CBCT scans of the maxilla, including the bilateral maxillary sinuses and the orbital floor up to the lower border of the maxillary alveolar process, with erupted incisors, canines, and premolars were selected. The total sample size was found to be at least 294 according to the power analysis (Critical $\chi^2 = 50.9985$, total sample size = 294, actual power = 0.8011).

The exclusion criteria were as follows: underage patients, artifacts preventing the evaluation of anatomical structures, missing tooth, implant and graft, supernumerary/impacted tooth, the presence of lesion in the anterior maxilla, maxillary surgery, syndrome or malformation, and poor quality CBCT scans. A total of 2327 CBCT images, including the maxilla, were examined. 568 CBCT images meeting the inclusion criteria were assessed.

The CBCT images were obtained using a Planmeca Promax 3D Mid (Planmeca, Helsinki, Finland) device with 16.0 × 9.2 cm FOV, 90 kVp, 12 mA, 13.5 sec, 0.4 mm voxel, or 16.0 × 16.3 cm FOV, 90 kVp, 12 mA, 13.5 sec, 0.4 mm voxel. The images were displayed with the original software Romexis 4.6.2.R (Planmeca, Helsinki, Finland) of the CBCT device. All images were analyzed on the same 24-inch medical monitor (Philips, Luchu Hsiang, Taiwan) with an ideal screen display (resolution: 1920 × 1080 pixels) provided with an NVIDIA QUADRO FX 380 graphics card. All examinations in the study were carried out by a researcher in the Department of Oral and Maxillofacial Radiology, in a quiet environment with reduced light, and approximately 50 cm away from the monitor. The brightness and contrast of the images were adjusted with the image manipulation tool in the computer software for optimum visualization. Axial, coronal, and sagittal planes were aligned to ensure standardization before the images were evaluated.

CBCT scanning to identify the CS and associated AC was performed according to the anatomical descriptions stated

in the previous literature (3,18,19). Studies on the visibility of canals in the anterior maxilla at different slice thicknesses have shown that optimal visualization is achieved at 0.5 mm and 1 mm slice thickness (20). In this study, axial, sagittal, coronal, and cross-sectional images with 0.5 mm slice thicknesses were used to evaluate the presence of CS and associated ACs. All images were scanned in the inferior direction from the border of the orbital floor to the lower border of the alveolar process, and in the horizontal direction from the midline to the distal of the premolar teeth.

First, the presence of CS was evaluated. The largest diameter measured in the axial sections formed from the origin of the CS to the termination of its course was accepted as the diameter of the CS (19,21). Second, the presence of an AC in the anterior maxilla was examined in patients with CS. Structures suspected to be ACs but smaller than 0.5 mm in diameter were excluded from the evaluation. The AC location was increased by modifying the regions given as reference in De Oliveira-Santos et al. (18). ACs were localized according to adjacent teeth (according to the FDI tooth numbering system) and incisive foramen.

It has been reported that the ASAN shows different variations in its course and number (22-24) thus, the trunk number of CS containing ASAN was evaluated as a single trunk or multiple trunks in coronal, sagittal, and axial sections in CBCT images with a slice thickness of 0.5 mm.

Chi-square analysis was used to examine the differentiation of the two categorical variables. In examining the differentiation of a continuous variable at the level of the categorical variable, the assumption of normal distribution was first evaluated. Unrelated sample t-test was used when the normal distribution was achieved, and the categorical variable level was two. In cases where the normal distribution was not achieved, the Mann-Whitney U test was used when the categorical variable level was two, and the Kruskal-Wallis H test was used when the categorical variable level was more than two. P value was taken as .05.

3. RESULTS

CBCT images belonging to 568 patients (240 males, and 328 females) were assessed. The ages of the participants ranged from 18 to 81 years (mean:42.51, standard deviation±14.43). Ages were grouped as 18-29, 30-39, 40-49, 50-59 and ≥ 60. The number of patients in the age groups was similar in terms of gender ($p > .05$). CS diameter according to age groups is shown in Table 1.

Table 1. Canalis sinuosus diameter (mm) in age groups

Age	18-29 Median (Min.-Max.)	30-39 Median (Min.-Max.)	40-49 Median (Min.-Max.)	50-59 Median (Min.-Max.)	≥60 Median (Min.-Max.)
Right	2.00 (1.13-4.33)	2.00 (1.13-4.33)	2.26 (0.89-4.00)	2.15 (1.13-3.96)	2.00 (1.13-4.56)
Left	2.00 (1.13-4.33)	2.15 (1.13-3.42)	2.15 (1.20-4.00)	2.26 (1.13-3.77)	2.02 (0.89-3.69)

*Kruskal Wallis H-Test

Min: Minimum Max: Maximum

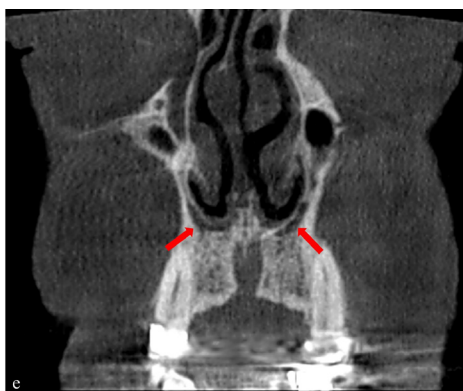
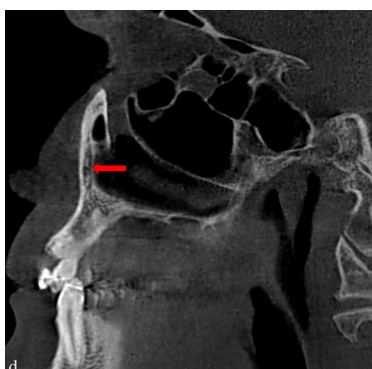


Figure 1. CBCT (cone-beam computed tomography) images of the CS (Canalis sinuosus) course; a-c) The axial plane, d) The sagittal plane, and e, f) The coronal plane. c, d, and f) CBCT images showing double trunk CS

Bilateral CS was detected in all patients (Figure 1). 91% of the CS on the right side had a single trunk, while 9% had a double trunk. Similarly, on the left side, 92% of the CS had a single trunk, while 8% had a double trunk. There was no significant difference between the right and left CS diameters of the patients ($p > .05$). When CS diameters were examined in terms of gender, both right and left CS diameters were larger in males than in females ($p < .001$, Table 2).

Table 2. Canalis sinuosus diameter (mm) and gender

Gender	Female Median (Min.-Max.)	Male Median (Min.-Max.)	Z'	p
Right	2.00 (1.13-3.96)	2.26 (0.89-4.56)	6.199	.000
	Female $\bar{X} \pm ss$	Male $\bar{X} \pm ss$	t**	p
Left	2.06±0.49	2.34±0.59	6.033	.000

*Mann Whitney U-Test

**Independent Sample T-Test

Min: Minimum Max: Maximum

In total, ACs were found in 238 (41.9%) patients (135 females, 103 males). 182 ACs were present in 135 females and 158 ACs were present in 103 males. A total of 340 ACs were found in the entire sample. One up to five ACs were seen in the patients. The majority of the females and males had one AC. Details are shown in Table 3.

Table 3. Presence of accessory canals according to gender

Total accessory canal number	Right (n %)		Left (n %)		Total (n %)	
	Female	Male	Female	Male	Female	Male
1	87 (%26.7)	67 (%27.9)	61 (%18.8)	47 (%19.6)	90 (%27.3)	63 (%26.3)
2	10 (%3)	10 (%4.2)	7 (%2.1)	9 (%3.8)	44 (%13.6)	29 (%12.1)
3	0 (%0)	2 (%0.8)			0 (%0)	8 (%3.3)
4					1 (%0.3)	2 (%0.8)
5					0 (%0)	1 (%0.4)

N: Number

A total of 340 ACs were detected, including at least one AC in 41.9% of the patients (Figure 2). AC diameter was between 0.5-1 mm in 70.9% of the patients and bigger than 1 mm in 29.1% of the patients. The median values of AC diameter in females were calculated as 0.89 mm (range=0.57–1.70 mm) and 0.89 mm (range=0.57–2.00 mm) on the right and left sides, respectively. In males, median values of the AC diameter were calculated as 0.89 mm (range=0.57–2.00 mm) and 0.89 mm (range=0.57–1.27 mm) on the right and left sides, respectively. Both the right and left AC diameters did not show a statistically significant difference according to the gender and age of the patients ($p > .05$, Table 4).

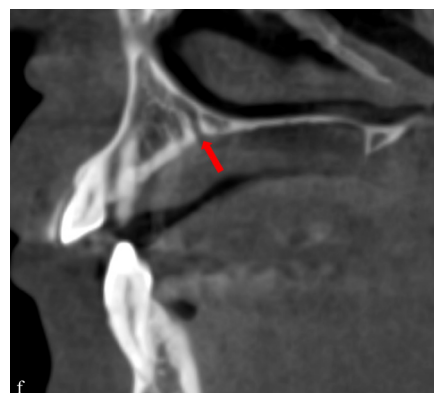
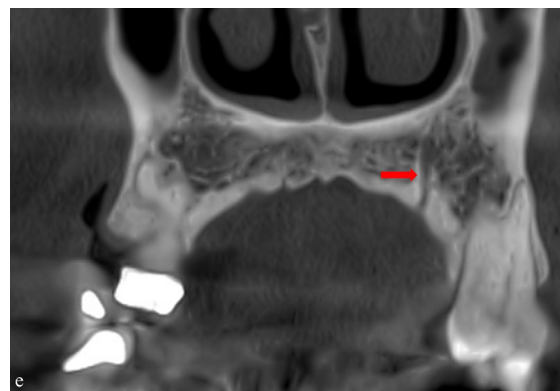
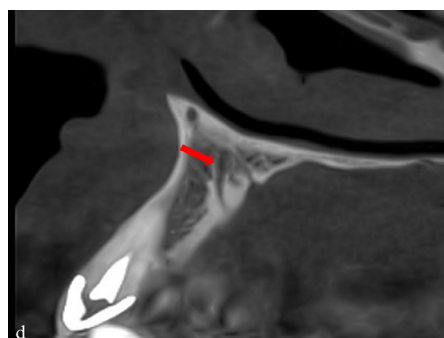
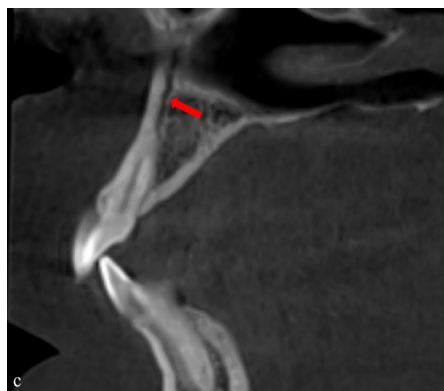
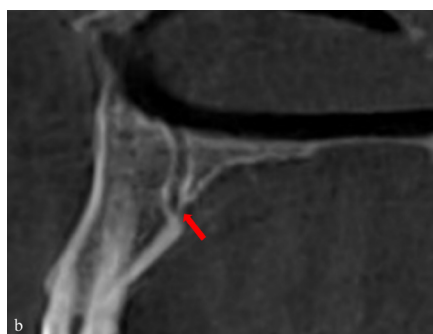
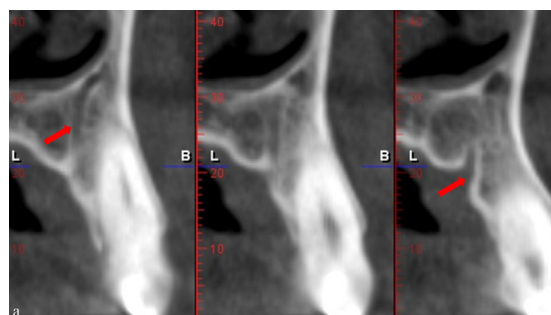


Figure 2. Cropped CBCT (cone-beam computed tomography) images of different patients showing the course of AC (accessory canal)

Table 4. Accessory canal diameter (mm) according to gender and age

Age/Gender	18-29	30-39	40-49	50-59	≥60	χ^2 (sd = 4)	p
	Median (Min.-Max.)	Median (Min.-Max.)	Median (Min.-Max.)	Median (Min.-Max.)	Median (Min.-Max.)		
Female	Right 0.89 (0.57-1.65)	0.89 (0.69-1.70)	0.80 (0.57-1.60)	0.87 (0.57-1.70)	0.89 (0.80-1.20)	4.332	.363
	Left 0.89 (0.57-1.65)	1.06 (0.57-1.65)	0.89 (0.57-1.26)	0.89 (0.57-2.00)	0.85 (0.57-1.26)		
Male	Right 0.89 (0.57-1.60)	0.89 (0.57-2.00)	0.89 (0.57-1.27)	0.89 (0.57-1.44)	0.89 (0.57-1.34)	.442	.979
	Left 0.80 (0.73-1.26)	0.89 (0.57-1.20)	0.80 (0.80-1.26)	0.89 (0.57-1.27)	0.80 (0.57-1.26)		

*Kruskal Wallis H test

Min: Minimum Max: Maximum

ACs were mostly located at tooth region 11 (17.9%), tooth region 12 (16.4%), tooth region 21 (13.8%), tooth region 22 (10.9%), and the anterior of the incisive foramen (10.6%). Details are shown in Table 5. All ACs did not have a radiographically observed foramen. 137 AC ended in the alveolar process or near the tooth roots and 203 AC ended with a foramen in the palatal, buccal or connected to the nasopalatine canal (NPC). A foramen was detected only in 59.71% of the ACs. 49.12% of the ACs had a palatal foramen, 1.47% had a buccal foramen, and 9.12% were associated with NPC (Table 6).

Table 5. Number of the accessory canals according to location in maxilla

Location*	Number of accessory canals
11	61 (%17.9)
Between 11-12	27 (%7.9)
12	56 (%16.4)
Between 12-13	6 (%1.8)
13	18 (%5.3)
Between 13-14	2 (%0.6)
14	0 (%0.0)
21	47 (%13.8)
Between 21-22	19 (%5.6)
22	37 (%10.9)
Between 22-23	6 (%1.8)
23	14 (%4.1)
Between 23-24	3 (%0.9)
24	1 (%0.3)
Anterior of the incisive foramen	36 (%10.6)
Posterior of the incisive foramen	0 (%0.0)
Lateral of the incisive foramen	7 (%2.1)
Total	340 (%100)

*Teeth are numbered according to the FDI system

Table 6. Accessory canals foramen and its location

Location of accessory canals foramen*	Location of foramen			
	Presence of foramen	Palatal	Buccal	Nasopalatine canal
11	38 (%11.18)	29 (%8.53)	1 (%0.29)	8 (%2.35)
Between 11-12	15 (%4.41)	15 (%4.41)	0 (%0.0)	0 (%0.0)
12	28 (%8.24)	28 (%8.24)	0 (%0.0)	0 (%0.0)
Between 12-13	4 (%1.18)	4 (%1.18)	0 (%0.0)	0 (%0.0)
13	16 (%4.71)	15 (%4.41)	1 (%0.29)	0 (%0.0)
Between 13-14	2 (%0.59)	2 (%0.59)	0 (%0.0)	0 (%0.0)
14	0 (%0.0)	0 (%0.0)	0 (%0.0)	0 (%0.0)
21	22 (%6.47)	17 (%5.00)	0 (%0.0)	5 (%1.47)
Between 21-22	12 (%3.53)	12 (%3.53)	0 (%0.0)	0 (%0.0)
22	24 (%7.06)	24 (%7.06)	0 (%0.0)	0 (%0.0)
Between 22-23	4 (%1.18)	4 (%1.18)	0 (%0.0)	0 (%0.0)
23	13 (%3.82)	12 (%3.53)	1 (%0.29)	0 (%0.0)
Between 23-24	3 (%0.88)	3 (%0.88)	0 (%0.0)	0 (%0.0)
24	1 (%0.29)	1 (%0.29)	0 (%0.0)	0 (%0.0)
Anterior of the incisive foramen	16 (%4.71)	1 (%0.29)	2 (%0.59)	13 (%3.82)
Posterior of the incisive foramen	0 (%0.0)	0 (%0.0)	0 (%0.0)	0 (%0.0)
Lateral of the incisive foramen	5 (%1.47)	0 (%0.0)	0 (%0.0)	5 (%1.47)
Total	203 (%59.71)	167 (%49.12)	5 (%1.47)	31 (%9.12)

*Teeth are numbered according to the FDI system

4. DISCUSSION

Periapical and panoramic radiographs, which are frequently used in dentistry, often can't describe, and show structures such as CS in detail (8,25). In particular, with the increase in the use of CBCT, better visualization of bony canals has caused CS to attract attention. There is great variation in the prevalence of CS due to the use of different methodologies in studies. (17,19,23,25-29).

Manhães junior et al. (25) detected CS in 36.20% of the patients, Aoki et al. (19) detected CS in 66.5% of the patients and Wanzeler et al. (27) detected this anatomic structure in 88% of the patients in CBCT scans. In our study, the entire course of CS after separation from the ION was comprehensively evaluated and the presence of bilateral CS was detected in the entire sample regardless of age and gender. Ghandourah et al. (29), Baena-Caldas et al. (28) and Gurler et al. (26) reported similar findings. In contrast, Aoki et al. (19) and Manhães junior et al. (25) reported a lower prevalence because they evaluated the prevalence of continuing CS only in the maxillary anterior region. In previous cadaver studies, researchers stated that ASAN could be of dual origin (22,23). In a study conducted with panoramic radiographs by Scarfe et al. (24) it was mentioned that the anterior superior dental plexus can be dual and triple. Some studies mention the presence of bifurcation and trifurcation during the course of CS (28). Radiological studies investigating the CS trunks are limited and usually mention the presence of furcation (28). In cadaver studies, the presence of ASAN with multiple trunks has been shown (22,23).

In our study, CS was evaluated in terms of the presence of single and multiple trunks in CBCT images. According to our results, 91% of the right side CS had a single trunk, while 9% had a double trunk. Similarly, on the left side, 92% of the CS showed a single trunk, while 8% showed a double trunk. The fact that the studies by Heasman (22) and Robinson and Wormald (23) were cadaver studies may explain the difference in the CS trunk pattern compared with our study.

As far as we know, there is no clear data describing the CS diameter in the literature. Jones described the CS as a bony canal approximately 2 mm in diameter and mentioned that the ASAN is at least one-third the size of the main trunk (6). Heasman stated that the diameter of the ASAN is between one-half, and one-third of the ION and that the ASAN is a larger structure than both the posterior superior alveolar nerve and the medial superior alveolar nerve (22). Gurler et al. (26) found no statistically significant difference in canal diameter according to age but, significantly higher mean canal diameters in males compared to females. In our study, both right and left CS diameters showed a statistically significant difference according to gender. A larger CS diameter in males may be related to wider anatomical structures in males than in females (26).

Radiographically visible ACs can contain neurovascular structures (3,18,30,31). Various designations have been used in the literature for these canals, including the lateral

incisive canal (32), neurovascular anatomical variations in the anterior palate (18), AC (3), and terminal extension of the CS.

In studies conducted with CBCT, the prevalence of AC in the anterior maxilla was found to be 27.8% by Von Arx et al. (3), 15.7% by De Oliveira-Santos et al. (18), 51.7% by Machado et al. (33), and 32.9% by Temmerman et al. (34). In studies conducted in the Turkish population, the prevalence of AC was found to be 22.3% by Sekerci et al. (35), 70.8% by Orhan et al. (36), 34.66% by Tomrukçu et al. (31), 8.17% by Şalli and Öztürkmen (37), and 35.5% by Alkis et al. (38). In our study AC were observed in 41.9% of the sample. Von Arx et al. (3) used limited CBCT images and evaluated canals with a minimum diameter of 1 mm. Temmerman et al. (34) examined only the canine region in their study. The fact that the area examined in these two studies is more limited than in our study may explain the higher prevalence of ACs in our study. De Oliveira-Santos et al. (18) and Sekerci et al. (35) evaluated patients with an additional foramen of the palate at least 1 mm in diameter. In our study, ACs associated with CS with diameter greater than 0.5 mm were evaluated. This may explain the higher prevalence of AC in our study compared with studies evaluating canals larger than 1 mm in diameter. In addition, the different prevalence seen in the studies may be due to the different methods used by the researchers, different device and imaging features, the variability of voxel sizes and examination areas, and the examination of patient populations with different ethnic origins.

Von Arx et al. (3) found the mean diameter of the AC as 1.31 mm (median=1.23 mm, range=1.01–2.13±0.26 mm) and that gender and age did not significantly affect the diameter. De Oliveira-Santos et al. (18) measured the palatal foramen opening of the canal in the anterior palate and found the mean diameter to be 1.4 mm (range=1–1.9 mm). Machado et al. (33) found that the mean diameter of the AC was 1.19 mm (median=1.15 mm, range=1.00–2.58±0.22 mm). In this study, the relationship between age and the number of ACs, the relationship between age and the diameter of the ACs, and the relationship between the number of ACs and gender were found to be feeble (33). Sekerci et al. (35) found that the mean diameter was 1.12 mm (range=1–1.7±0.26 mm). In these studies, only the diameter of canals with a diameter greater than 1 mm was measured. Tomrukçu et al. (31) found a median diameter of 1.07 mm (range=0.53–2.72±0.35 mm) for AC with a diameter greater than 0.5 mm. In Machado et al. (33), 20% of the ACs was at least 1 mm in diameter. In our study, 70.9% of the ACs had a diameter between 0.5 and 1 mm, while 29.1% had a diameter of 1 mm or more. In our study, there was no statistically significant difference in the diameter of both the right and left AC according to gender and age.

In the study by De Oliveira-Santos et al. (18), most of the ACs were observed in the alveolar process near to the incisor or canine teeth. Sekerci et al. (35) found that ACs were most commonly located on the palatal of the left and right lateral incisors. Tomrukçu et al. (31) found ACs most frequently in the right lateral incisor region. The researchers found

that the regions with the lowest number of ACs were the region between teeth 14 and 15 and between teeth 24 and 25 (31). Machado et al. (33) found that the ends of the AC trajectories were most frequently located in the palatal region of the anterior maxillary teeth and less frequently in the buccal and transversal positions. Of the ACs in our study, 49.12% had palatal foramen and 1.47% had buccal foramen. Previous studies have reported that the presence of ACs was associated with NPC (18,35). In our study, 9.12% of the ACs were associated with the NPC.

59.71% of the ACs had a foramen, whereas 40.29% of the ACs terminated in the apical region or around the tooth roots in the alveolar process. In our study, not only canals with palatal openings but also all ACs were associated with CS in the anterior maxilla. The voxel size in this study was 0.4 mm. This voxel size is larger than many studies, which may have limited the visualization of the terminal portions of the ACs. Additionally, most studies have evaluated canals of only 1 mm or larger (3,18,35). ACs with a diameter of less than 1 mm were also evaluated in our study. This may also have allowed the evaluation of ACs smaller than 1 mm in diameter terminating around tooth roots.

Within the CS is the anterior superior alveolar vascular nerve bundle. While cadaver studies focused more on ASAN, radiological studies focused on the prevalence, course, and variations of CS. The limitation of this study was the examination of only CBCT images of the patients.

5. CONCLUSION

In conclusion, all patients had CS on both the right and left side of the cranium. ACs were in nearly half of the patients. Insufficient knowledge about these structures may lead to misdiagnosis and complications during surgical procedures. For this reason, physicians should know the major anatomical structures and the variations.

Acknowledgements: This manuscript is a part of the thesis of Hatice Tetik entitled "Investigation of Canalis Sinuosus and Related Accessory Canals in Cone-Beam Computed Tomography Images"

Funding: The authors received no financial support for the research.

Conflicts of interest: The authors declare that they have no conflict of interest.

Ethics Committee Approval: This study was approved by Ethics Committee of Gazi University, (Approval date: 07.01.2020; Number: 91610558-604.01.02-)

Peer-review: Externally peer-reviewed.

Author Contributions: (Initials only)

Research idea: HT, ZA

Design of the study: HT, ZA

Acquisition of data for the study: HT

Analysis of data for the study: HT, ZA

Interpretation of data for the study: HT, ZA

Drafting the manuscript: HT

Revising it critically for important intellectual content: HT, ZA

Final approval of the version to be published: HT, ZA

REFERENCES

- [1] White SC, Pharoah MJ. *Oral Radiology: Principles and Interpretation*. 7th ed. St. Louis, Missouri: Mosby Elsevier; 2014.
- [2] Özdede M, Paksoy CS. Konik ışınli bilgisayarlı tomografi: teknik, çalışma ilkeleri ve görüntü oluşumu. *Türkiye Klinikleri J Oral Maxillofac Radiol-Special Topics*. 2019;5(1):1-6. (Turkish)
- [3] Von Arx T, Lozanoff S, Sendi P, Bornstein MM. Assessment of bone channels other than the nasopalatine canal in the anterior maxilla using limited cone beam computed tomography. *Surg Radiol Anat*. 2013;35(9):783-790. DOI: 10.1007/s00276.013.1110-8
- [4] Rodella LF, Buffoli B, Labanca M, Rezzani R. A review of the mandibular and maxillary nerve supplies and their clinical relevance. *Arch Oral Biol*. 2012;57(4):323-334. DOI: 10.1016/j.archoralbio.2011.09.007
- [5] Liang X, Lambrichts I, Corpas L, Politis C, Vrielinck L, Ma GW, Jacobs R. Neurovascular disturbance associated with implant placement in the anterior mandible and its surgical implications: Literature review including report of a case. *Chin J Dent Res*. 2008;11(1):56-64.
- [6] Jones FW. The anterior superior alveolar nerve and vessels. *Journal Anat*. 1939;73(Pt 4):583-591.
- [7] Lester Mc Daniel WM. Variations in nerve distributions of the maxillary teeth. *Journal Dent Res*. 1956;35(6):916-921. DOI: 10.1177/002.203.4556035.006.1301
- [8] Shelley AM, Rushton VE, Horner K. Canalis sinuosus mimicking a periapical inflammatory lesion. *Br Dent J*. 1999;186(8):378-379. DOI: 10.1038/sj.bdj.4800116
- [9] Leven AJ, Sood B. Pathosis or additional maxillary neurovascular channel? A case report. *J Endod*. 2018;44(6):1048-1051. DOI: 10.1016/j.joen.2018.02.025
- [10] Talim JS, Schechter D, Roges R, Rotstein I. Canalis sinuosus mimicking root resorption lesion. *Endodontology*. 2018;30(2):140-143.
- [11] Shah PN, Arora AV, Kapoor SV. Accessory branch of canalis sinuosus mimicking external root resorption: A diagnostic dilemma. *J Conserv Dent*. 2017;20(6):479-481.
- [12] Shintaku WH, Ferreira CF, de Souza Venturin J. Invasion of the canalis sinuosus by dental implants: A report of 3 cases. *Imaging Sci Dent*. 2020;50(4):353-357. DOI: 10.5624/isd.2020.50.4.353
- [13] Arruda JA, Silva P, Silva L, Álvares P, Silva L, Zavanelli R, Rodrigues C, Gerbi M, Sobral AP, Silveira M. Dental implant in the canalis sinuosus: A case report and review of the literature. *Case Rep Dent*. 2017;2017:4810123. DOI:10.1155/2017/4810123
- [14] Volberg R, Mordanov O. Canalis sinuosus damage after immediate dental implant placement in the esthetic zone. *Case Rep Dent*. 2019 Dec 16:2019:3462794. DOI: 10.1155/2019/3462794
- [15] Ananthaneni A, Srilekha N, Guduru VS, Kiresur MA. Rare case report of traumatic neuroma of anterior superior alveolar nerve associated with high frenal attachment. *Asian J Neurosurg*. 2015;10(2):169-171. DOI: 10.4103/1793-5482.153502
- [16] Dorafshar AH, Dellon AL, Wan EL, Reddy S, Wong VW. Injured anterior superior alveolar nerve endoscopically resected within maxillary sinus. *Craniofacial Trauma Reconstr*. 2017;10(3):208-211. DOI: 10.1055/s-0036.159.2088
- [17] Olenczak JB, Hui-Chou HG, Aguila III DJ, Shaeffer CA, Dellon AL, Manson PN. Posttraumatic midface pain: Clinical significance of the anterior superior alveolar nerve and canalis sinuosus. *Ann Plast Surg*. 2015;75(5):543-547. DOI: 10.1097/SAP.000.000.0000000335
- [18] De Oliveira-Santos C, Rubira-Bullen IRF, Monteiro SAC, Leon JE, Jacobs R. Neurovascular anatomical variations in the anterior palate observed on CBCT images. *Clin Oral Implants Res*. 2013;24(9):1044-1048. DOI: 10.1111/j.1600-0501.2012.02497.x
- [19] Aoki R, Massuda M, Zenni LTV, Fernandes KS. Canalis sinuosus: Anatomical variation or structure? *Surg Radiol Anat*. 2020;42(1):69-74. DOI: 10.1007/s00276.019.02352-2
- [20] Anatoly A, Sedov Y, Gvozdikova E, Mordanov O, Kruchinina L, Avanesov K, Vinogradova A, Golub S, Khaydar D, Hoang NG, Darawsheh HM. Radiological and morphometric features of canalis sinuosus in russian population: Cone-beam computed tomography study. *Int J Dent*. 2019 Dec 16:2019:2453469. DOI:10.1155/2019/2453469
- [21] Etöz M, Yılmaz S. Anterior palatal açıklığı olan canalis sinuosus varyasyonları. *Türkiye Klinikleri J Dent Sci*. 2019;25(3):241-247. (Turkish)
- [22] Heasman PA. Clinical anatomy of the superior alveolar nerves. *Br J Oral Maxillofac Surg*. 1984;22(6):439-447. DOI:10.1016/0266-4356(84)90051-2
- [23] Robinson S, Wormald PJ. Patterns of innervation of the anterior maxilla: A cadaver study with relevance to canine fossa puncture of the maxillary sinus. *Laryngoscope*. 2005;115(10):1785-1788. DOI: 10.1097/01.mlg.000.017.6544.72657.a6
- [24] Scarfe WC, Langlais RP, Ohba T, Kawamata A, Maselle I. Panoramic radiographic patterns of the infraorbital canal and anterior superior dental plexus. *Dentomaxillofac Radiol*. 1998;27(2):85-92.
- [25] Manhães Júnior LRC, Villaça-Carvalho MFL, Moraes MEL, Lopes SLPDC, Silva MBF, Junqueira JLC. Location and classification of canalis sinuosus for cone beam computed tomography: Avoiding misdiagnosis. *Brazil Oral Res*. 2016;30(1):e49. DOI: 10.1590/1807-3107BOR-2016.vol30.0049
- [26] Gurler G, Delilbasi C, Ogut EE, Aydin K, Sakul U. Evaluation of the morphology of the canalis sinuosus using cone-beam computed tomography in patients with maxillary impacted canines. *Imaging Sci Dent*. 2017;47(2):69-74. DOI: 10.5624/isd.2017.47.2.69
- [27] Wanzeler AMV, Marinho CG, Junior SMA, Manzi FR, Tuji FM. Anatomical study of the canalis sinuosus in 100 cone beam computed tomography examinations. *Oral Maxillofac Surg*. 2015;19(1):49-53. DOI: 10.1007/s10006.014.0450-9
- [28] Baena-Caldas GP, Rengifo-Miranda HL, Herrera-Rubio AM, Peckham X, Zúñiga JR. Frequency of canalis sinuosus and its anatomic variations in cone beam computed tomography images. *Int J Morphol*. 2019;37(3):852-857.
- [29] Ghandourah AO, Rashad A, Heiland M, Hamzi BM, Friedrich RE. Cone-beam tomographic analysis of canalis sinuosus accessory intraosseous canals in the maxilla. *Ger Med Sci*. 2017 Dec 19:15:Doc20. DOI: 10.3205/000261
- [30] Neves FS, Crusoé-Souza M, Franco LCS, Caria PHF, Bonfim-Almeida P, Crusoé-Rebello I. Canalis sinuosus: A rare anatomical variation. *Surg Radiol Anat*. 2012;34(6):563-566. DOI: 10.1007/s00276.011.0907-6
- [31] Tomrukçu DN, Köse TE. Assessment of accessory branches of canalis sinuosus on CBCT images. *Med Oral Patol Oral Cir Bucal*. 2020;25(1):e124-e130. DOI: 10.4317/medoral.23235

- [32] Vâlcu M, Rusu MC, Sendroiu VM, Didilescu AC. The lateral incisive canals of the adult hard palate-aberrant anatomy of a minor form of clefting. *Rom J Morphol Embryol.* 2011;52(3):947-949.
- [33] Machado VC, Chrcanovic BR, Felipe MB, Manhães Júnior LRC, de Carvalho PSP. Assessment of accessory canals of the canalis sinuosus: A study of 1000 cone beam computed tomography examinations. *Int J Oral Maxillofac Surg.* 2016;45(12):1586-1591. DOI: 10.1016/j.ijom.2016.09.007
- [34] Temmerman A, Hertelé S, Teughels W, Dekeyser C, Jacobs R, Quirynen M. Are panoramic images reliable in planning sinus augmentation procedures? *Clin Oral Implants Res.* 2011;22(2):189-194. DOI: 10.1111/j.1600-0501.2010.02000.x
- [35] Sekerci AE, Cantekin K, Aydınbelge M. Cone beam computed tomographic analysis of neurovascular anatomical variations other than the nasopalatine canal in the anterior maxilla in a pediatric population. *Surg Radiol Anat.* 2015;37(2):181-186. DOI: 10.1007/s00276.014.1303-9
- [36] Orhan K, Görürgöz C, Akyol M, Özarslanturk S, Avsever H. An anatomical variant: Evaluation of accessory canals of the canalis sinuosus using cone beam computed tomography. *Folia Morphol.* 2018;77(3):551-557. DOI: 10.5603/FM.a2018.0003
- [37] Şallı GA, Öztürkmen Z. Evaluation of location of canalis sinuosus in the maxilla using cone beam computed tomography. *Balk J Dent Med.* 2021;25(1):7-12.
- [38] Alkis HT, Ata GC, Tas A. Evaluation of the morphology of accessory canals of the canalis sinuosus via cone-beam computed tomography. *J Stomatol Oral Maxillofac Surg.* 2023;124(4):101406. DOI: 10.1016/j.jormas.2023.101406

How to cite this article: Tetik H, Akarslan Z. Anatomical Variations of the Canalis Sinuosus: A CBCT Study. *Clin Exp Health Sci* 2024; 14: 835-842. DOI: 10.33808/clinexphealthsci.1443811